Theor Appl Climatol (2011) 106:443–448
DOI 10.1007/s00704-011-0450-8

ORIGINAL PAPER

Why do 2-day waves propagate westward?

Fei Liu · Gang Huang · Licheng Feng

Received: 18 February 2011 / Accepted: 16 April 2011 / Published online: 28 April 2011

Abstract In observations, the 2-day waves, identified as the convectively coupled equatorial inertio-gravity (IG) waves, only propagate westward. To understand this feature, a simple theoretical model is presented for the convectively coupled equatorial waves (CCEWs). Under the assumption that the convective heating is proportional to the vertical velocity on the first baroclinic mode, the nonlinear governing equation for the meridional velocity of the CCEWs can be derived. The optimal method is used to obtain the dispersion relation from this nonlinear equation, and the results show that the deep convection can slow down the IG waves by decreasing the mean state static stability, but the key leading to the westward propagation of the IG waves is the full meridional variation of the sea surface temperature (SST). The warm SST trapped near the equator excites long westward propagating IG waves, whereas the warm SST trapped near the ITCZ centered at 10° N excites short westward propagating IG waves. This theoretical model provides a simple tool to study the CCEWs in understanding the tropical circulation.

F. Liu
International Pacific Research Center,
University of Hawai'i at Manoa,
Honolulu, HI 96822, USA

G. Huang
Key Laboratory of Regional Climate-Environment Research
for Temperate East Asia, Institute of Atmospheric Physics,
Chinese Academy of Sciences,
Beijing 100029, China

G. Huang (✉)
State Key Laboratory of Numerical Modeling for Atmospheric
Sciences and Geophysical Fluid Dynamics, Center for Monsoon
System Research, Institute of Atmospheric Physics,
Chinese Academy of Sciences,
Beijing 100083, China
e-mail: hg@mail.iap.ac.cn

L. Feng
National Marine Environmental Forecasting Center,
Beijing 100081, China

1 Introduction

1.1 Properties of 2-day waves

The 2-day waves feature the zonal wavelength of 2,000–4,000 km and westward propagation of 10–30 ms^{-1} convective systems with a life cycle of about 2 days (Takayabu 1994a; Takayabu et al. 1996; Haertel and Johnson 1998; Haertel and Kiladis 2004; Haertel et al. 2008), which mainly occur in the equatorial western Pacific during the northern winter (Takayabu 1994a). Actually, many 2-day waves prevail during the active phase of the Madden–Julian Oscillation (MJO) (Nakazawa 1988; Hendon and Liebmann 1994; Madden and Julian 1994; Schrage et al. 2001; Clayson et al. 2002) and are important to modify the low-frequency eastward propagating Kelvin waves (Kikuchi and Wang 2010) and even the MJO (Biello and Majda 2005; Kikuchi and Wang 2010).

1.2 Equatorial waves associated with the 2-day waves

High-resolution soundings of the Tropical Ocean Global Atmosphere Coupled Ocean–atmosphere Response Experiment (TOGA COARE) have given chances to explore the complex feature of the 2-day waves: the shallow convection phase associated with congestus clouds leading the initial tower and mature phase associated with deep convective cloud, and then the decaying phase associated with stratiform clouds (Takayabu et al. 1996). The multi-cloud

structure has explained (Haertel and Kiladis 2004; Haertel et al. 2008) why the dispersion characteristics of 2-day waves resemble those of classical shallow-water equatorial waves (Matsuno 1966) with equivalent depths of 12–50 m (Emanuel et al. 1994; Takayabu 1994b; Mapes 2000; Majda and Shefter 2001; Lindzen 2003; Majda and Biello 2004). The first baroclinic vertical mode associated with the deep convective heating has an equivalent depth of about 50 m, while the second baroclinic vertical mode associated with congestus and stratiform has an equivalent depth of one fourth of the first mode, about 12.5 m (Haertel and Kiladis 2004). Albeit its complex structure, the spectral signal of 2-day waves usually lies along the dispersion curve for the n=1 westward propagating inertio-gravity (IG) waves (Takayabu 1994a; Takayabu et al. 1996; Wheeler and Kiladis 1999). The horizontal structure from TOGA COARE also indicates that the 2-day waves are controlled by the n=1 westward propagating IG waves, although they have complex vertical structures (Takayabu et al. 1996; Haertel and Kiladis 2004).

1.3 Why do 2-day waves usually move westward?

The dry equatorial IG waves show both eastward and westward propagation (Matsuno 1966), whereas the 2-day waves always propagate westward (Takayabu 1994a; Takayabu et al. 1996; Haertel and Johnson 1998; Haertel and Kiladis 2004; Haertel et al. 2008). Why do the 2-day waves only propagate westward? Not only the symmetric but also the anti-symmetric IG waves propagate westward. Actually the eastward propagating equatorial convective systems can only be related to the equatorial Kelvin and n=0 mixed Rossby-gravity waves (Wheeler and Kiladis 1999; Kiladis et al. 2009). The horizontal structures of 2-day waves, with the maximum clouds at the equator (Takayabu et al. 1996; Haertel and Kiladis 2004), show much accordance with those of the westward IG waves. This feature gives a hint to explain why the 2-day waves usually propagate westward.

In this paper, we will explain this westward propagation according to the spectrum of convectively coupled equatorial waves (CCEWs). Section 2 derives the model, and the mathematic method is presented in section 3. The model results are given in section 4, and section 5 gives the physical explanation. This paper ends with a discussion.

2 The model

Based on the moisture-stratiform instability (Kuang 2008), Andersen and Kuang (2008) built a toy model to study the instability of the CCEWs while their model is complicated. From the observations (Haertel and Kiladis 2004), the first baroclinic mode still dominates in the 2-day waves, and the first baroclinic diabatic heating can exceed three times that of the second baroclinic mode. So the first baroclinic mode can represent the deep convection of the 2-day waves very well (Haertel and Kiladis 2004), which provides an easy way to understand the 2-day waves. In this paper, we discuss the CCEWs based on the shallow-water equations on a β-plane (Matsuno 1966), but the diabatic heating is included in this model. Assuming that the equivalent height is h_e, so velocity, length, and time scales are $C_{\mathrm{ref}} = \sqrt{gh_e}$, $L_c = (C_{\mathrm{ref}}/\beta)^{1/2}$ and $T_c = (C_{\mathrm{ref}}\beta)^{-1/2}$, respectively, where $\beta = f_y = 2 \times 10^{-11}\mathrm{m}^{-1}\mathrm{s}^{-1}$($f$ is the Coriolis parameter). The nondimensional shallow-water equations can be written as

$$u_t - yv = -\phi_x, \tag{1}$$

$$v_t + yu = -\phi_y, \tag{2}$$

$$\phi_t + (u_x + v_y) = -Q, \tag{3}$$

where x and y represent the horizontal disturbances, t is time. u and v denote the x and y components of velocity. ϕ is the geopotential height, and Q is the diabatic heating. The diabatic heating can simply be represented by the moisture convergence (Wang 1988), and this relation has the observational support for the 2-day waves (Haertel and Kiladis 2004; Haertel et al. 2008),

$$Q = -b(y)(u_x + v_y), \tag{4}$$

where $b(y)$ is the mean state moisture parameter associated with the sea surface temperature (SST), which is larger on the warmer SST (Wang 1988). This study mainly focuses on the direction selection of the 2-day waves, so only the meridional variation of the moisture is considered.

We now seek solutions to Eqs. 1–4 of the form

$$(u, v, \phi) = R_e[U(y), V(y), \Phi(y)]e^{i(kx-\sigma t)}, \tag{5}$$

Where k and σ are the wavenumber and frequency, respectively. By substituting Eq. 5 into Eqs. 1–4, we can obtain the governing equation for $V(y)$ only

$$F(k,\sigma) = V_{yy} - \frac{a_y}{a}V_y + \left[\frac{1}{(b-1)}y^2 + \frac{a_y}{a\sigma}ky - \frac{1}{\sigma}k - a\right]V = 0, \tag{6}$$

where

$$a = \frac{\sigma^2}{(b-1)} + k^2, \quad a_y = -\frac{\sigma^2 b_y}{(b-1)^2}. \tag{7}$$

3 Optimal solution

For the dry equatorial waves, $b(y)=0$, Eq. 6 reduces to the well-known equation for the equatorial waves (Matsuno 1966) and the dispersion relation can be obtained easily. For the CCEWs, $b(y)>0$, it is hard to find an analytical solution for Eq. 6. While for the given meridional structures of $V(y)$ and $b(y)$, we can obtain the optimal solution of Eq. 6, which is determined by the function of

$$O(F) = 1/\left(\frac{1}{2y_b}\int_{-y_b}^{y_b} F\mathrm{d}y\right), \tag{8}$$

Where $-y_b$ and y_b are the south and north boundaries, respectively, and $y_b=50°$ in this paper, and the experiments show that the selection of the meridional band (y_b) does not affect the results. In all four figures of this paper, the normalized $O(F)$, divided by the maximum value of each experiment, is plotted in the wavenumber-frequency filed, where the bigger the $O(F)$ is, the better the solution becomes, and the equatorial waves are more easy to occur at that wavenumber and frequency. For the analytical solutions, $O(F)=1$ along the analytical dispersion curves.

Following Matsuno's work (Matsuno 1966), the meridional (y) structure of the waves is given in terms of parabolic cylinder function (D), which takes the form

$$D_n(y/y_0) = \exp\left[-(y/y_0)^2\right]P_n(y/y_0), \tag{9}$$

Where P_n is a polynomial of degree n, and y_0 is the trapping scale given by $y_0=L_c$. The meridional structure of the $b(y)$ takes the form of

$$b = b_0 D_0[(y-y_c)/L_b), \tag{10}$$

Where y_c is the latitude of the SST center, L_b is the trapping scale of the SST. Equation 10 means that the SST is trapped at latitude y_c with a trapping scale of L_b, and b_0 is the amplitude, which is usually less than 1 (Wang 1988).

4 Results for the n = 1 IG waves

When the $V_{(y)}$ takes the anti-symmetric structure with respect to the equator, D_1, which represents the IG or the Rossby waves. Here we only discuss the IG waves, and the Rossby waves are not talked about in this paper. Our results show that the dispersion curves (red lines in Fig. 1) are the same with the analytical solutions of Matsuno (1966) for the dry IG ($n=1$) waves (upper pattern in Fig. 1), and even for the Rossby waves (lower pattern in Fig. 1), which means that this model is reliable. We only consider the convectively coupled IG waves with the same equivalent length of 50 m. When $b_0=0$, Fig. 1 shows that the dry IG waves (the brown shade) can propagate eastward or westward in accordance with the analytical result. But when the diabatic heating is included ($b_0>0$), the IG waves mainly propagate westward with a period of about 2 days, represented by the blue shade for a cool SST, $b_0=0.3$, and by the green shade for a warm SST, $b_0=0.6$. Usually, the diabatic heating slows down the dry equatorial waves, but why the convectively coupled IG waves

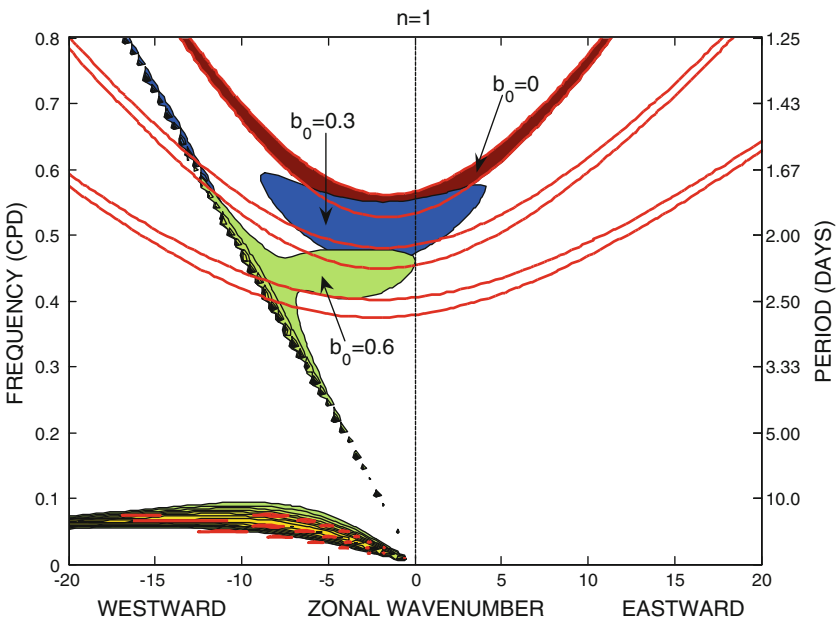

Fig. 1 Dispersion curves for the $n=1$ dry equatorial waves (*red lines*), which are plotted for the equivalent depths of 12, 25, 50 m. The curves are plotted when $O(F)>0.99$. The shades are plotted for the equatorial waves without coupled heating (*brown shade*, $b_0=0$), with a cool SST (*blue shade*, $b_0=0.3$), and with a warm SST (*green shade*, $b_0=0.6$), respectively. In all shades, the equivalent depth is 50 m, $y_c=0$ and $L_b=L_c$. The *brown shade* is plotted when $O(F)>0.99$ while the *blue* and *green shades* are plotted when $O(F)>0.8$

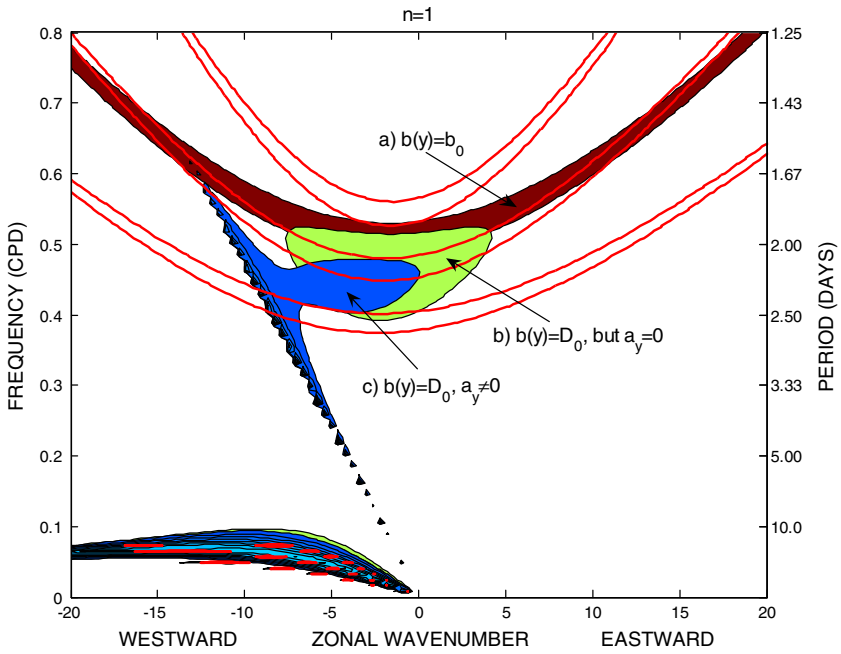

Fig. 2 Curves are the same as in Fig. 1. Shades are plotted for the equatorial waves with different meridional SST centered at the equator: **a** constant SST (*brown shade*, $b=b_0$); **b** polarward decaying SST (*green shade*, $L_b=L_c$ and $a_y=0$); **c** full polarward decaying SST (*blue shade*, $L_b=L_c$ and $a_y\neq0$). In all shades, the equivalent depth is 50 m, $b_0=0.6$ and $y_c=0$. The *brown shade* is plotted when $O(F)>0.99$, while the *blue* and *green shades* are plotted when $O(F)>0.8$

only move westward is still unclear. (Note: the dot line in the left part of the shade is the characteristic line where $a\rightarrow0$, and the numerical solution by this method will be singular there.)

To understand why the convectively coupled IG waves always propagate westward, we further study them with different meridional structures of SST centered at the equator. Here, we take a warm SST, $b_0=0.6$ as in Fig. 1. Three meridional cases are studied in Fig. 2: (a) constant SST (brown shade), which has no meridional variation, $b=b_0$; (b) polarward decaying SST (green shade), which has the trapping scale of $L_b=L_c$, but in this case we omit the terms including a_y in Eq. 6, as done by Lindzen (1974); and (c) full polarward decaying SST (blue shade), which is the same as in (b) but $a_y\neq0$. Fig. 2 shows that when the full meridional variation of the SST is considered, the IG waves can only propagate westward (blue shade of Fig. 2). Although Lindzen (1974) gave the most unstable IG mode for the ITCZ, his work could not explain why the IG waves only propagate westward, and the IG waves can still propagate eastward in his case (green shade in Fig. 2).

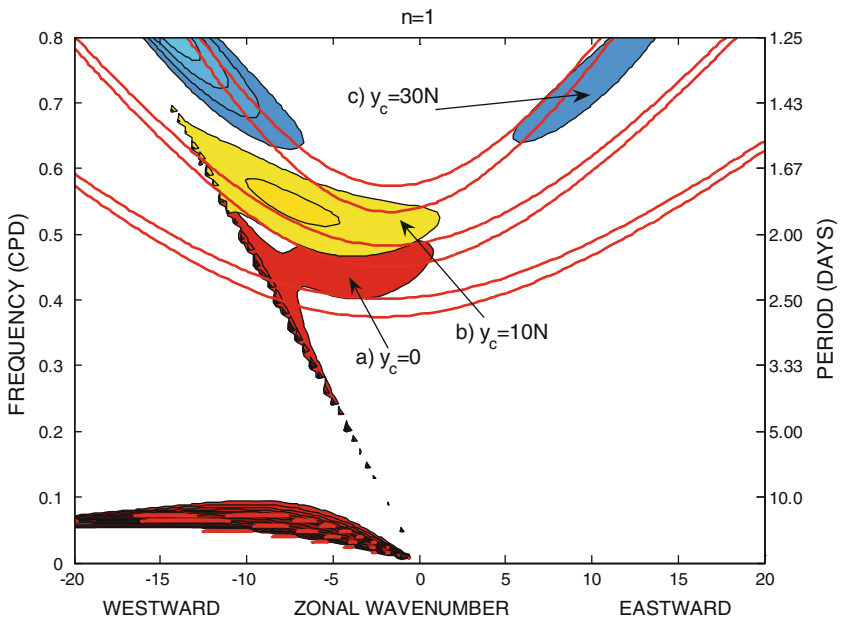

Fig. 3 Curves are the same as in Fig. 1. Shades are plotted for the equatorial waves with different SST center, where the SST is centered at **a** the equator (*red shade*), **b** 10° N (*yellow shade*), and **c** 30° N (*blue shade*), respectively. In all shades, the equivalent depth is 50 m, $b_0=0.6$ and $L_b=L_c$. All shades are plotted when $O(F)>0.8$

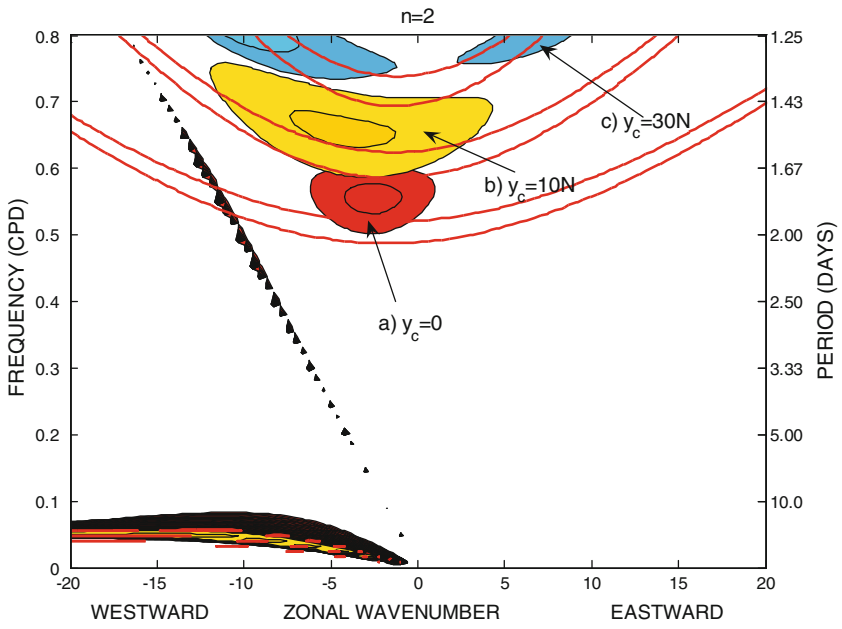

Fig. 4 Same as in Fig. 3, but for the n=2 IG waves

In Fig. 3, the location of the SST center also affects the propagating properties of the IG waves. When the warm SST is centered at the equator and decays polarward, the IG waves only propagate westward, but have a long wavelength, with a wavenumber smaller than 5 (red shade in Fig. 3); for the ITCZ case, where the warm SST is centered at 10° N, the IG waves show a more obvious westward propagation, and they prefer short waves, with wavenumber of 5~10 (yellow shade in Fig. 3); the high latitude warm SST will excite high frequency IG waves which can propagate westward or eastward (blue shade in Fig. 3), although such a SST pattern is unrealistic.

5 Physical explanation

Figures 1 and 2 show that IG waves coupled with the equatorial-trapped convection will propagate westward. This can be understood from the meridional structure of dry IG waves, for n=1, the analytical meridional structure of the vertical velocity is $\frac{c_0}{C_{\mathrm{ref}}k-\sigma}D_2 + \frac{c_0}{C_{\mathrm{ref}}k+\sigma}D_0$, where C_0 is the amplitude. For the westward propagating IG waves, k<0, $|c_0/(C_{\mathrm{ref}}k-\sigma)| < |c_0/(C_{\mathrm{ref}}k+\sigma)|$, and the meridional structure is dominated by D_0; while for the eastward propagating IG waves, the meridional structure is dominated by D_2. Usually above the ocean, the mean state moisture, in phase with the SST, has its biggest projection on D_0, which has a maximum value near the equator (Wang 1988). So the westward propagating IG waves will be enhanced while the eastward propagating IG waves will be damped.

6 Conclusions

The theoretical model presented here provides a simple tool to understand why the 2-day waves, the convectively coupled IG waves only move westward: the deep convection can slow down the IG waves by decreasing the mean state static stability, but the key leading to the westward propagation of IG waves is the full meridional variation of the SST. The warm SST trapped near the equator will excite long westward propagating IG waves while the warm SST trapped near the ITCZ will excite short westward propagating IG waves.

Observations show that the IG waves on the high mode (n=2) also propagate westward (Wheeler and Kiladis 1999). When taking the n=2 structure in this model, Fig. 4 still gives the same results as Fig. 3, but long IG waves are preferred when compared with the n=1 waves, which is in accord with the observation (Wheeler and Kiladis 1999).

The simple theoretical model provides a new tool to study the CCEWs. It can be useful to study tropical circulation. In the future works, the role of the boundary layer Ekman pumping and high baroclinic modes should also be implemented into this simple model to give a more reasonable explanation.

Acknowledgements This work was supported by the National Basic Research Program of China (2011CB309704), Special Scientific Research Project for Public Interest (grant no. GYHY201006021), and the National Natural Science Foundation of China (grant nos. 40890155, 40775051, U0733002, 40906014, and 40976015).

References

Andersen J, Kuang Z (2008) A toy model of the instability in the equatorially trapped convectively coupled waves on the equatorial Beta plane. J Atmos Sci 65:3736–3757

Biello JA, Majda AJ (2005) A new multiscale model for the Madden–Julian oscillation. J Atmos Sci 62:1694–1721

Clayson CA, Strahl B, Schrage JM (2002) 2–3-day convective variability in the tropical western Pacific. Mon Weather Rev 130:529–548

Emanuel KA, Neelin JD, Bretherton CS (1994) On large-scale circulations in convecting atmospheres. Q J R Meteorol Soc 120:1111–1143

Haertel PT, Johnson RH (1998) Two-day disturbances in the equatorial western Pacific. Q J R Meteorol Soc 124:615–636

Haertel PT, Kiladis GN (2004) On the dynamics of 2-day equatorial disturbances. J Atmos Sci 61:2707–2721

Haertel PT, Kiladis GN, Denno A, Rickenbach T (2008) Vertical mode decompositions of 2-day waves and the Madden–Julian oscillation. J Atmos Sci 65:813–833

Hendon HH, Liebmann B (1994) Organization of convection within the Madden–Julian oscillation. J Geophys Res 99:8073–8083

Kikuchi K, Wang B (2010) Spatiotemporal wavelet transform and the multiscale behavior of the Madden–Julian oscillation. J Climate 23:3814–3834

Kiladis, G. N., M. C. Wheeler, P. T. Haertel, K. H. Straub, and P. E. Roundy, 2009: Convectively coupled equatorial waves. Rev. Geophys., 47, RG2003.

Kuang Z (2008) A moisture-stratiform instability for convectively coupled waves. J Atmos Sci 65:834–854

Lindzen RS (1974) Wave-CISK in the tropics. J Atmos Sci 31:156–179

Lindzen RS (2003) The interaction of waves and convection in the tropics. J Atmos Sci 60:3009–3020

Madden R, Julian P (1994) Observations of the 40–50-day tropical oscillation—a review. Mon Weather Rev 122:814–837

Majda AJ, Biello JA (2004) A multiscale model for the intraseasonal oscillation. Proc Natl Acad Sci USA 101:4736–4741

Majda AJ, Shefter MG (2001) Models for stratiform instability and convectively coupled waves. J Atmos Sci 58:1567–1584

Mapes BE (2000) Convective inhibition, subgrid-scale triggering energy, and stratiform instability in a toy tropical wave model. J Atmos Sci 57:1515–1535

Matsuno T (1966) Quasi-geostrophic motions in the equatorial area. J Meteorol Soc Jpn 44:25–43

Nakazawa T (1988) Tropical super clusters within intraseasonal variations over the western Pacific. J Meteorol Soc Jpn 66:823–839

Schrage JM, Clayson CA, Strahl B (2001) Statistical properties of episodes of enhanced 2–3-day convection in the Indian and Pacific oceans. J Climate 14:3482–3494

Takayabu YN (1994a) Large-scale cloud disturbances associated with equatorial waves. Part II: westward propagating inertio-gravity waves. J Meteorol Soc Jpn 72:451–465

Takayabu YN (1994b) Large-scale cloud disturbances associated with equatorial waves. Part I: spectral features of the cloud disturbances. J Meteorol Soc Japan 72:433–448

Takayabu YN, Lau KM, Sui CH (1996) Observation of a quasi-2-day wave during TOGA COARE. Mon Weather Rev 124:1892–1913

Wang B (1988) Dynamics of tropical low-frequency waves: an analysis of the moist Kelvin wave. J Atmos Sci 45:2051–2065

Wheeler M, Kiladis GN (1999) Convectively coupled equatorial waves: analysis of clouds and temperature in the wavenumber-frequency domain. J Atmos Sci 56:374–399